Midbrain–hindbrain involvement in lissencephalies

Patrice Jissendi-Tchofo, MD
Simay Kara, MD
A. James Barkovich, MD

Address correspondence and reprint requests to Dr. Patrice Jissendi-Tchofo, Radiology Department, Erasme Hospital, Route de Lennik 808, B-1070 Brussels, Belgium
jissendi@gmail.com

ABSTRACT

Objectives: To determine the involvement of the midbrain and hindbrain (MHB) in the groups of classic (cLIS), variant (vLIS), and cobblestone complex (CBSC) lissencephalies and to determine whether a correlation exists between the cerebral malformation and the MHB abnormalities.

Methods: MRI scans of 111 patients (aged 1 day to 32 years; mean 5 years 4 months) were retrospectively reviewed. After reviewing the brain involvement on MRI, the cases were reclassified according to known mutation (*LIS1*, *DCX*, *ARX*, *VLDLR*, *RELN*, *MEB*, *WWS*) or mutation phenotype (*LIS1-P*, *DCX-P*, *RELN-P*, *ARX-P*, *VLDLR-P*) determined on the basis of characteristic MRI features. Abnormalities in the MHB were then recorded. For each structure, a score was assigned, ranging from 0 (normal) to 3 (severely abnormal). The differences between defined groups and the correlation between the extent of brain agyria/pachygyria and MHB involvement were assessed using Kruskal–Wallis and χ^2 McNemar tests.

Results: There was a significant difference in MHB appearance among the three major groups of cLIS, vLIS, and CBSC. The overall score showed a severity gradient of MHB involvement: cLIS (0 or 1), vLIS (7), and CBSC (11 or 12). The extent of cerebral lissencephaly was significantly correlated with the severity of MHB abnormalities ($p = 0.0029$).

Conclusion: Our study focused on posterior fossa anomalies, which are an integral part of cobblestone complex lissencephalies but previously have not been well categorized for other lissencephalies. According to our results and the review of the literature, we propose a new classification of human lissencephalies. *Neurology*® 2009;72:410–418

GLOSSARY

A = autosomal; **ACC** = agenesis of corpus callosum; **AD** = autosomal dominant; **AP** = anteroposterior; **AR** = autosomal recessive; **CBL** = cerebellar; **CBSC** = cobblestone complex; **cLIS** = classic lissencephaly; **CMD** = congenital muscular dystrophy; **CSZ** = cell-sparse zone; **DV** = dorsal–ventral; **FCMD** = Fukuyama congenital muscular dystrophy; **IVH** = inferior vermis hypoplasia; **LV** = lateral ventricle; **m** = medulla; **M** = midbrain; **MDS** = Miller–Dieker syndrome; **MEB** = muscle–eye–brain; **MHB** = midbrain and hindbrain; **MR** = magnetic resonance; **ND** = not determined; **P** = pons; **RC** = rostrocaudal; **SCBH** = subcortical band heterotopia; **SELH** = subependymal linear heterotopia; **V** = vermis; **vLIS** = variant lissencephaly; **WI** = weighted image; **WWS** = Walker–Warburg syndrome; **XLD** = X-linked dominant; **XLR** = X-linked recessive.

The term *lissencephaly* (smooth outer brain surface) refers to a paucity of gyral and sulcal development.[1] It encompasses a spectrum of gyral malformations ranging from complete agyria to regional pachygyria and includes subcortical band heterotopia. Lissencephaly has been traditionally classified in two distinct groups: classic (cLIS, formerly called *lissencephaly type 1*) and cobblestone complex (CBSC, formerly called *lissencephaly type 2*) based on both brain imaging and pathology. To date, five genes have been identified as causing or contributing to human cLIS: *LIS1*, *14-3-3ε* in Miller–Dieker syndrome (MDS), *DCX*, *RELN*, and *ARX*.[1-6] A new classification has recently been proposed defining four groups of cLIS differing from each other by genetics and neuropathologic features of the cerebral cortex, cerebellum, and brainstem.[3] 1)

Supplemental data at www.neurology.org

Editorial, page 394

e-Pub ahead of print on November 19, 2008, at www.neurology.org.
From the Neuroradiology section (P.J.-T., S.K., A.J.B.), Department of Radiology, University of California, San Francisco, CA; Service de Neuroradiologie (P.J.-T.), Hôpital R. Salengro, Centre Hospitalier Régional de Lille, France; Neuroradiology section (P.J.-T.), Department of Radiology, Erasme Hospital, Brussels, Belgium; and Department of Radiology (S.K.), Faculty of Medicine, Kirikkale University, Turkey.
Supported by R37 NS035129 from the National Institute of Neurological Disorders and Stroke, NIH, Bethesda, MD.
Disclosure: The authors report no disclosures.

LIS1 mutations and MDS show a four-layered cortex predominantly posterior with white matter heterotopia in the cerebellum, a normal three-layered cerebellar cortex, and normal to small pons. 2) *DCX* mutations show a four-layered cortex similar to *LIS1* but predominantly anterior; cerebellar and pontine abnormalities are similar to those in *LIS1* mutations. 3) *ARX* mutations have a three-layered cortex; the cerebellum is normal, but the pons is small due to hypoplastic corticospinal tracts. 4) Lissencephaly with a two-layered cortex, diffuse involvement of the brain surface with no gradient; the cerebellum is extremely hypoplastic with pontine and medullary disorganization. No *RELN*-like mutations were studied. The authors divided these lissencephalies into two groups: *LIS1* and *DCX* were classified as cLIS, whereas *ARX* and two-layered lissencephalies were classified as variant lissencephaly (vLIS).[3]

Numerous genes have been identified in association with the CBSC (also called *dystroglycanopathies*).[7-12] Most affected patients have symptoms of congenital muscular dystrophies (CMDs) with CNS involvement. Among these disorders, three phenotypes are well defined: Fukuyama congenital muscular dystrophy (FCMD), Walker–Warburg syndrome (WWS), and muscle–eye–brain disease (MEB).[1,7-11] These phenotypes have been associated with mutations of multiple genes involved in *O*-glycosylation of α-dystroglycan, including *FCMD*, *FKRP*, *POMT1*, *POMT2*, *LARGE*, and *POMGnT1*.[12]

The aim of our study was to determine the involvement of the midbrain and hindbrain (MHB) in these disorders, and to determine whether a correlation exists between the cerebral malformation and the MHB characteristics as determined by MRI.

METHODS MRI scans or portions of MRI scans of 120 patients were retrospectively reviewed. The scans were acquired from the private teaching collection of the senior author (acquired over 22 years), from the teaching file of the radiology department at our institution (searching using *lissencephaly*, *agyria*, *pachygyria*, *band heterotopia*, *cobblestone malformation*, and *congenital muscular dystrophy* as key words), and from MRIs reviewed for a study of the genetics of epilepsy. MRIs were only included if good quality images of the cerebrum (to assess the type and severity of the cortical malformation) and posterior fossa were available as determined by a consensus of the authors. Most studies included T1-weighted and T2-weighted images with scans performed in at least two planes. Four cases were excluded because only CT images were available and, therefore, assessment of the posterior fossa content was suboptimal. Five others were excluded because the posterior fossa structures were not assessed on magnetic resonance (MR) images available. The remaining 111 MRI studies were analyzed. Patients were aged 1 day to 32 years (mean 5 years 4 months; median 2 years) at the time of MRI, including 54 men, 41 women, and 16 with unavailable sex information. The MRIs included sagittal and axial T1-weighted, axial, and coronal T2-weighted images with slices of 3- to 5-mm thickness. Cases were classified as "lissencephalies" in the database according to the diagnosis based on brain MRI features or known genetics. Clinical information was not often available; when available, it was usually brief, reporting mental retardation and seizures and, sometimes, family history. After reviewing the brain involvement, the cases were reclassified according to known mutation (*LIS1*, *DCX*, *ARX*, *VLDLR*, *RELN*, *MEB*, *WWS*) or mutation phenotype (*LIS1-P*, *DCX-P*, *RELN-P*, *ARX-P*, *VLDLR-P*) according to characteristic MR features[1]; many of the patients were imaged before testing for specific mutations was available and were not able to be found; therefore, the number with a confirmed genetic diagnosis is low. Phenotypes were determined as follows:

- *LIS1-P*: agyria (absence of gyri) or pachygyria (few broad and flat gyri) more severe posteriorly (parietal and occipital lobes) than anteriorly with a thick cortex (10–15 mm), smooth brain surface, reduced white matter, and cell-sparse zone between a thin outer layer cortex and a thick inner layer of gray matter (figure 1A).
- *DCX-P*: the same features as in *LIS1-P* but more severe in anterior brain (frontal or frontocentral regions). Band heterotopia that was more severe in the frontal and frontoparietal regions was included in this group (figure 1C).
- *RELN-P*: thickened cortex (8–10 mm) with too few sulci, decreased hippocampal rotation, no cell-sparse zone.
- *ARX-P*: moderately thick cortex (5–7 mm) with undersulcation most severe in temporal and occipital lobes, absence of corpus callosum, and small, dysplastic basal ganglia. No *ARX-P* were identified in our database.
- Not determined (ND): no definite genetic diagnosis and features too non specific to propose a "probable" genetic diagnosis.

The *VLDLR* mutation was proposed (*VDLR-P*) for patients having the so-called dysequilibrium syndrome.[13,14] Patients with cLIS (*LIS1*, *LIS1-P*, *DCX*, *DCX-P*) were designated as cLIS, and those with *ARX*, *RELN*, *RELN-P*, and ND were designated as vLIS. All cases with defined mutations of *O*-glycosylation genes (*FKRP*, *POMGnT1*) and those without defined mutation (*CMD-P*) but features of CBSC on brain MRI were classified as CBSC. Cases not fitting the previously defined groups were considered to be a new group. We did not include *CMD* with Merosin deficiency in this study, because it does not manifest brain features of CBSC and is not of the group of disorders previously called type 2 lissencephaly.[15]

After this initial classification, the posterior fossa in each case was carefully reviewed with separate attention to the midbrain, the pons, the medulla, the cerebellar vermis, and the cerebellar hemispheres. Morphologic features were then recorded according to a systematic visual analysis as follows:

- Midbrain: dorsal–ventral (DV) and rostrocaudal (RC) size, tectal size, and collicular morphology.

Figure 1 Classic and variant lissencephalies

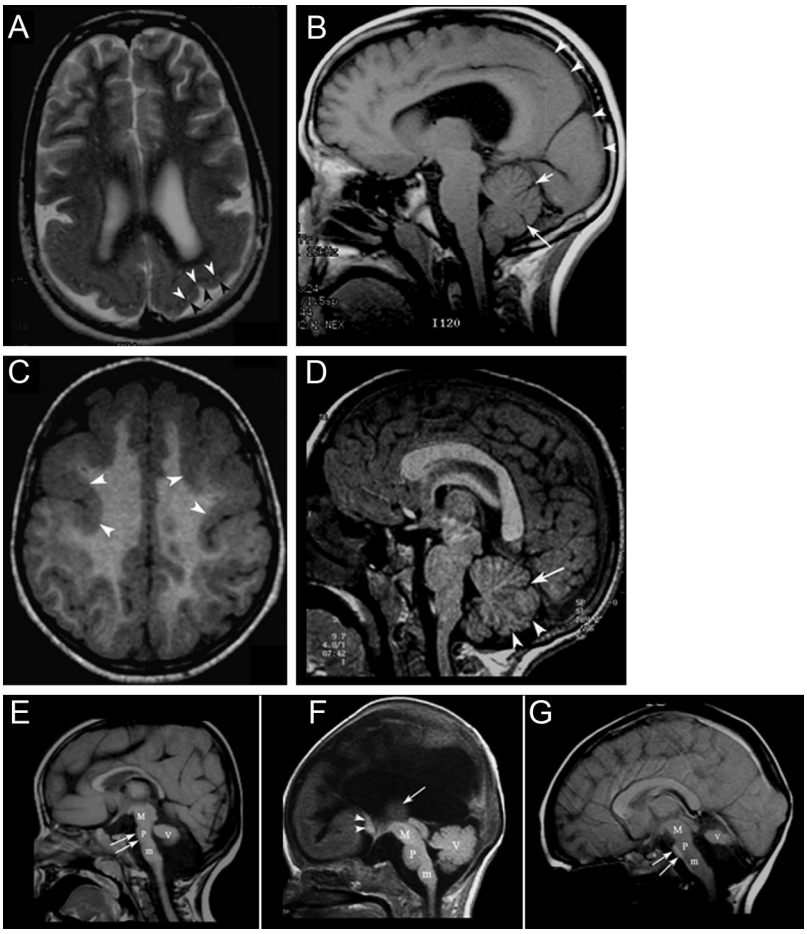

(A and B) Patient 2 with LIS1 mosaicism. Axial T2-weighted image (WI) (A) shows a pachygyria with a gradient that is worse posteriorly. The inner cortex is thick and separated from the outer thin layer (black arrowheads) by a cell-sparse zone (white arrowheads) that has signal intensity of myelinated white matter with some areas of hyperintensity. Sagittal T1WI (B) shows the smooth surface of the brain involving the posterior frontal, parietal, and occipital cortices (white arrowheads). In the posterior fossa, midbrain and hindbrain appear normal. The vermis is normal with visible primary fissure (short arrow) and prepyramidal fissure (long arrow) defining three parts in equal proportions. (C and D) Patient 34 with DCX mutation. Axial T1WI (C) shows a thick cortex with few broad gyri (white arrowheads) that are worse anteriorly. On the sagittal T1WI (D), the inferior vermis (arrowheads) appears small compared with the anterior vermis (limited posteriorly by the primary fissure [arrow]). The other posterior fossa structures are normal. (E) Patient 61 with presumed *RELN* mutation having the same brain magnetic resonance features as his female sibling (patient 59) in whom *RELN* mutation was found. On sagittal T1WI, pachygyria is worse anteriorly, the midbrain (M) is small, and the pons (P) is hypoplastic, resulting in the flattening of its ventral aspect (double arrows). The medulla (m) is mildly hypoplastic, whereas the vermis is severely hypoplastic. (F) Patient 54 with *ARX* mutation. Sagittal T1WI shows agenesis of the corpus callosum with prominent anterior commissure (arrowheads), small basal ganglia (arrow), hypoplastic midbrain (M), pons (P) and medulla (m), and hypoplastic and dysplastic vermis (V). (G) Patient 89, from a Hutterite family, having dysequilibrium syndrome and *VLDLR* mutation. Sagittal TIWI shows same features of midbrain and hindbrain involvement as in RELN mutation (A), including a severe hypoplasia of the vermis (V) and cerebellar hemispheres.

- Pons and medulla: DV and RC size. *Hypoplasia* refers to loss of pontine anterior curvature and small ventral pons.
- Cerebellar vermis: Anteroposterior (AP) and RC size. *Hypoplasia* refers to a small vermis showing a few or no fissures and no identifiable prepyramidal fissure; *dysplasia* refers to abnormal foliation or disorientation of fissures. The presence or absence of cysts was noted.
- Cerebellar hemispheres: overall size and fissures. Hypoplasia, dysplasia, and cysts were defined with same criteria as for the vermis.

The degree of involvement was further characterized as mild or severe, based on consensus by the authors.

For statistics, a score was assigned for each main feature: normal = 0; mildly hypoplastic (including inferior vermis hypoplasia) = 1; severely hypoplastic (including vermian hypoplasia) = 2; dysplastic (including cerebellar and vermian cysts as well as pontomedullary "kink") = 3. To assess the differences between defined groups of patients based on MHB features and to evaluate the correlation between the brain agyria/pachygyria and MHB involvement, nonparametric statistical tests were used, Kruskal–Wallis test for multiple group comparison and χ^2 McNemar test (Statistica version 7.1, StatSoft France, 2005, www.statsoft.fr). A p value less than 0.05 was considered significant.

RESULTS Table e-1 (on the *Neurology*® Web site at www.neurology.org) shows all patients included in the study listed by number, sex, and age, and classified according to lissencephaly groups and genotype/phenotype. For each patient, corresponding forebrain, midbrain, and hindbrain involvement are reported.

Table 1 summarizes the results of the statistical tests. Only significant p values are reported to show group differences. The discriminating MR feature makes the difference between groups for each MHB structure. Significant differences were found between cLIS and vLIS, and between cLIS and CBSC. Moreover, according to the predefined score assignment, we found a severity gradient of MHB involvement.

Normal mid-hindbrain was found in 85% of cLIS patients, including all *LIS1*, 60% of *LIS1-P*, 50% of *DCX*, and 58% of *DCX-P* (figure 1, A and B). Moderate mid-hindbrain involvement corresponded to isolated inferior vermis hypoplasia (IVH), small or hypoplastic vermis, cerebellar hemispheres, midbrain, pons, or medulla. Among the cLIS patients with IVH, 75% were either *DCX* or *DCX-P* (in equal proportions) (figure 1, C and D). Severe mid-hindbrain involvement included severe hypoplasia or dysplasia of the vermis and cerebellar hemispheres, cysts within the vermis and cerebellar hemispheres, midbrain hypoplasia or dysplasia, severe hypoplasia of the pons and medulla, pontomedullary kink, and pontine midline cleft. These features were remarkably predominant among the vLIS (figure 1, E–G) and CBSC groups, differentiating them significantly from cLIS groups (table 1). Interestingly, all patients with *WWS* phenotype had a ventral midline pontine cleft associated with severe hindbrain hypoplasia (figure 2).

We found an association between agyria/pachygyria of the entire brain (with or without gradient) and severe MHB involvement ($p = 0.0029$).

Table 1 Statistical analyses

Structure	Discriminating MRI feature	Group differences	*p* Value (<0.05)	Group score for MHB involvement								
				cLIS		vLIS			CBSC			
				LIS1-P	*DCX-P*	*ARX*	*RELN-P*	VLDLR-P	*CMD-P*	*MEB*	*WWS*	ND
CBL vermis	Hypoplasia and dysplasia	*ARX* =/ *DCX-P*	0.036295	0	0 or 1	3	2	2	3	3	2	2
	Hypoplasia and dysplasia	*CMD-P* =/ *DCX-P*	0.012228									
CBL hemispheres	Severe hypoplasia	*VLDLR-P* =/ *DCX-P*	0.018496	0	0	1	2	2	3	3	2	0
	Dysplasia-cysts	*CMD-P* =/ *LIS1-P*	0.041018									
	Dysplasia-cysts	*CMD-P* =/ *DCX-P*	0.000452									
	Severe hypoplasia	*WWS* =/ *DCX-P*	0.002345									
Midbrain	Mild hypoplasia	*VLDLR-P* =/ *LIS1-P*	0.021621	0	0	1	1	1	3	1 or 3	3	0
	Dysplasia-large tectum	*CMD-P* =/ *LIS1-P*	0.003119									
	Dysplasia-large tectum	*CMD-P* =/ *DCX-P*	0.013815									
	Dysplasia-large tectum	*WWS* =/ *LIS1-P*	0.000008									
	Dysplasia-large tectum	*WWS* =/ *DCX-P*	0.000112									
	Dysplasia-large tectum	*WWS* =/ ND	0.005544									
Pons	Mild hypoplasia	*CMD-P* =/ *DCX-P*	0.030652	0	0	1	1	1	1	1	3	0
	Severe hypoplasia-dysplasia	*WWS* =/ *LIS1-P*	0.000006									
	Severe hypoplasia-dysplasia	*WWS* =/ *DCX-P*	0.000001									
	Pontomedullary "kink"	*WWS* =/ ND	0.006137									
Medulla	Mild hypoplasia	*VLDLR-P* =/ *DCX-P*	0.022306	0	0	1	1	1	1	1	2	1
	Severe hypoplasia	*WWS* =/ *LIS1-P*	0.000176									
	Severe hypoplasia	*WWS* =/ *DCX-P*	0.000039									
Total score				0	1	7	7	7	11	11	12	3

Significant *p* values for group differences and for each midbrain and hindbrain (MHB) structure. Discriminating MRI feature refers to the predominant feature within the first group cited in the "Group differences" column. Group score is the score corresponding to the predominant MRI feature (the most frequent in each group according to statistic histograms).
cLIS = classic lissencephaly; vLIS = variant lissencephaly; CBSC = cobblestone complex; ND = not determined; CBL = cerebellar.

Figure 2 Cobblestone complex in patient 107 with *WWS* phenotype

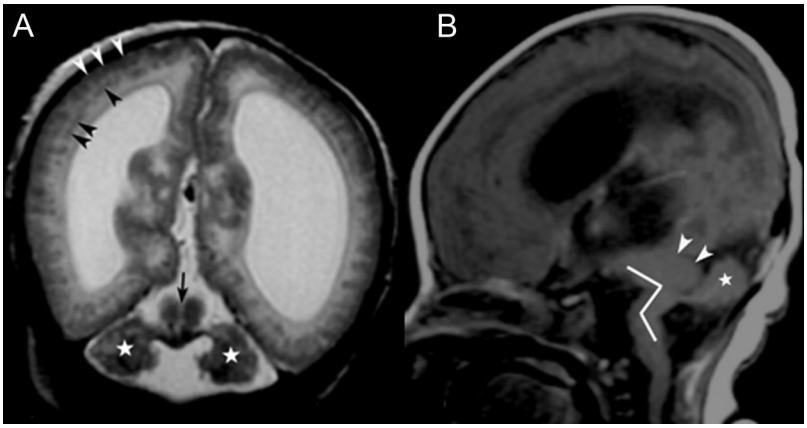

(A) Coronal T2-weighted image (WI) showing typical magnetic resonance appearance of cobblestone complex with irregular inner layer of ectopic neurons (black arrowheads) and overmigrated neurons at the surface of the cortex (white arrowheads) and between both fibroglial bundles crossing the white matter radially, hydrocephalus, and profound hypomyelination. Midbrain and hindbrain (white stars on cerebellar hemispheres) are severely hypoplastic with near total absence of the vermis and pontine midline cleft (black arrow). (B) Sagittal T1WI showing the characteristic dysplastic large tectum (arrowheads), deformity of the mid-hindbrain junction (pontomedullary "kink," white line), and near total absence of the vermis with very hypoplastic cerebellar hemisphere (white star).

Agenesis of corpus callosum (ACC) (1.27% of all lissencephalies) was always associated with severe involvement of the vermis; it was found in vLIS with no defined genotype, as expected in all *ARX* mutations, and in two patients with complete agyria and undulating band heterotopia (figure 3, A and B). In addition, periventricular nodular heterotopia was seen in patients with normal to mild MHB involvement and subependymal linear heterotopia (SELH) in two patients with near total absence of the vermis and hypoplastic pons (figure 3, C and D).

DISCUSSION This study used a database including many patients with lissencephalies to perform a systematic review of MHB structures in a large series including many types of lissencephalies. More than a simple, exploratory approach to the distribution of cerebellar and brainstem abnormalities in lissencephalies, this study tested whether a relationship existed between the type and extent of supratentorial involvement and the involvement of the mid-hindbrain, and whether, as hypothesized, the distribution among different defined groups could help to predict the mutation by associating the pattern of cerebral involvement with mid-hindbrain involvement.

The patterns of cerebral involvement have been well documented in human lissencephalies and have helped to classify them and to correlate them with histology and genetics.[1-10] Consistent differences were found in the gyral patterns among cLISs, with the malformation more severe posteriorly in individuals with *LIS1* mutations and more severe anteriorly in individuals with *DCX* mutations.[4] These observations were later correlated with neuropathologic findings as mentioned in the introduction.[3] The pattern of cortical brain involvement in cLIS is typically different from what is seen in "cobblestone malformations" associated with defects in *O*-glycosylation of α-dystroglycan.[7-11,16] The agyria/pachygyria complex seen in cLIS and vLIS is mainly the result of incomplete migration of neurons,[2-6] whereas CBSC is primarily a result of overmigration of neurons, many of which pass through gaps in the glial limiting membrane.[7-11] Involvement of the cerebellum and the pons has been described in cLISs that were classified according to mutation analysis. Some authors found hypoplasia of the cerebellar vermis to be more common in patients with *DCX* mutations, whereas both *DCX* and *LIS1* sometimes had normal cerebellum and brainstem.[4] The new pathologic classification recently proposed included cerebellum and brainstem abnormalities associated with cLIS (*LIS1* and *DCX*) and vLIS (*ARX* and two-layered cortex).[3] They found the most severe involvement of the hindbrain (hypoplasia) in vLIS group and, most notably, in two-layered cortex. In our series, the mid-hindbrain in cLIS ranged from normal to small (more frequently among *DCX* and *DCX-P* patients) in agreement with previous studies. Our observations were similar, revealing an association between the extent of brain involvement and severity of MHB abnormalities ($p = 0.0029$). Marked to severe MHB hypoplasia was most often found in patients with pachygyria involving the entire cerebrum, relatively thin cortex (5 mm or less), and no cell-sparse zone (vLIS-ND, likely Forman's two-layered cortex lissencephaly). As discussed by previously cited authors,[3] this association could be related to extensive impairment of cortical fibers projecting to the pons as well as hypoplasia of mid-hindbrain nuclei.

Of interest, we found a high rate of isolated inferior vermis hypoplasia associated with *DCX*. This sign is probably to be considered as the smallest degree of MHB involvement and would give an interesting clue for differential diagnosis if the finding is substantiated on subsequent studies. *MHB* was severely hypoplastic in *ARX* patients (with dysmorphic features of the vermis) and in patients with *RELN* mutations. Different phenotypes of lissencephaly with cerebellar hypoplasia (LCH) are associated with *LIS1*, *DCX*, and *RELN* genes.[6,17]

All patients initially classified as *VLDLR* and *VLDLR-P* had MHB features similar to patients with *RELN* mutation. Consequently, the two groups had the same overall score for MHB involvement (table 2). Severe hypoplasia of the vermis was found in all *RELN* (two cases) and in five of eight *VLDLR* and

Figure 3 Not-determined lissencephalies

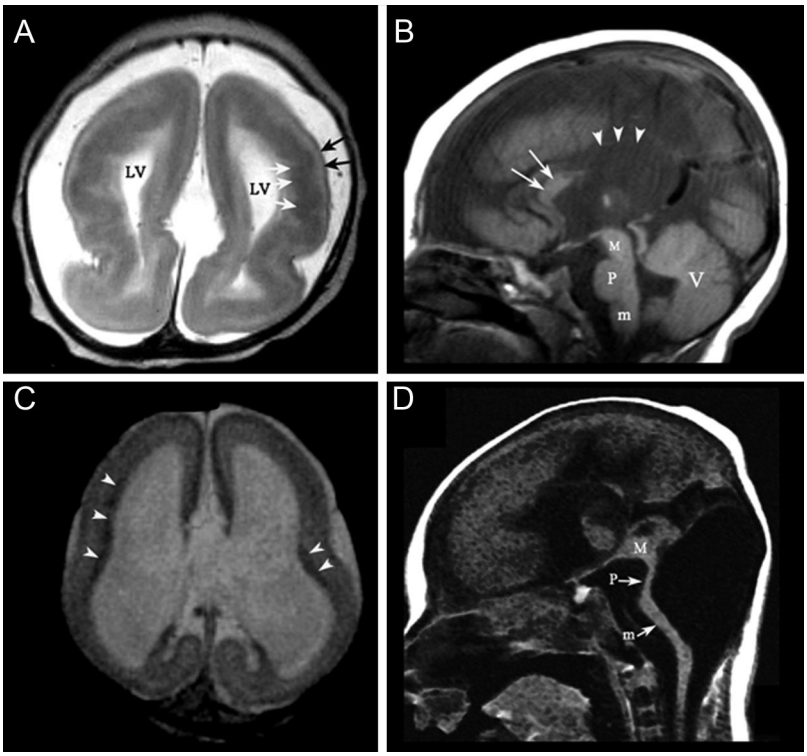

(A and B) Patient 67 classified as not determined (ND). Axial T2-weighted image (WI) (A) shows entire brain agyria with very thin outer cortex layer (black arrows) and undulating gray matter heterotopia (white arrows) surrounding the enlarged lateral ventricles (LVs). Sagittal T1WI (B) displays callosal hypogenesis with small posterior genu (white arrows) but absent body (arrowheads), with small midbrain (M), pons (P), and medulla (m), and enlarged dysplastic vermis. (C and D) Patient 78 classified as ND. Axial T2WI (C) shows agyria of the entire brain with subependymal linear gray matter heterotopia bilaterally (white arrowheads) and marked ventriculomegaly in this microcephalic patient. Sagittal T1WI (D) displays callosal agenesis and extremely hypoplastic midbrain (M), pons (P), and medulla (m). The entire cerebellum is nearly absent.

VLDLR-P patients. These were grouped together as vLIS. The *VLDLR* mutation has been described as responsible for the so-called dysequilibrium syndrome and can therefore be presumed in any patient with characteristic clinical and brain MRI features.[18]

CBSC was formerly called type 2 lissencephaly.[12] It is the main CNS feature of CMDs with *O*-glycosylation defects of α-dystroglycan, even though it is difficult to differentiate the genetic causes on the basis of brain MRI because of overlapping phenotypes.[19-23] Cerebral, cerebellar, and brainstem abnormalities have been well documented in the major phenotypes: *FCMD*, *WWS*, and *MEB*. *WWS* displays severe cerebral cortical dysplasia, hypomyelination, dysplastic tectum, pontomedullary kink, severe hypoplasia of the vermis, and dysplastic cerebellar hemispheres.[1,10] A ventral midline cleft of the ventral pons is often associated with *MEB* and *WWS* and could also be considered among their typical MR features. The midline cleft is probably due to reduced number of crossing pontine axons, possibly resulting from impaired tangential migration of pontine nuclei, as demonstrated in mice with mutation of *Large*.[24,25]

We found that callosal agenesis is not uncommon among patients with lissencephaly. ACC is among the characteristic features of *ARX*-associated lissencephaly.[26,27] The frequent association of ACC with vLIS-ND patients in our series suggests considering this feature as a supplementary criteria to differentiate cLIS from vLIS. It is important to note, however, that ACC may also be found in other types of lissencephalies.[28] Interestingly, the cerebellar vermis was dysplastic or severely hypoplastic in 13 of 14 patients with ACC; it will be interesting to see whether this association holds up in other series. A recent study of callosal agenesis associated with DCX found that the doublecortin protein might be involved in the early stages of corpus callosum formation[29]; however, none of the *DCX* or *DCX-P* patients in this study had ACC.

This study is limited by the small number of cases with established genetic diagnoses. An attempt was made to increase this number by assigning a presumed genetic classification based on established cerebral MRI features in different lissencephaly groups and correlation of imaging features with known pathologic features such as cell-sparse zones, associated callosal anomalies, and cortical thickness. This is obviously not scientifically rigorous and may be considered an artificial classification. However, we observed relative homogeneity of MHB involvement both within groups with presumed classification (*LIS1-P*) and between groups with known and presumed mutations of the same gene (*DCX*, *RELN*, and *VLDLR*). This homogeneity and our statistical results emboldened us to group together those with presumed and proved mutations for purposes of correlation. Results of these groupings are shown in the two first columns of table 2. For each structure analyzed, a gradient of involvement was found to be associated with each presumed genotype (mutation phenotype) (table e-2). We suggest that these presumed groupings might be useful to determine which tests for specific gene mutations should be performed in such patients.

Based on the data in this project and that in the literature, we propose a classification similar to that recently proposed,[3] separating cLIS (*LIS1* and *DCX*) from vLIS (*RELN* and *ARX*) (table 2). We included *VLDLR* and some ND cases with markedly atypical MR features, namely ND1, ND2, and ND3, within the vLIS group. ND3 refers to a case with microcephaly, paracentral pachygyria, and ACC resembling Baraitser–Winter syndrome, but other phenotypes may be associated with this syndrome.[30] ND2 refers to two cases with undulating band heterotopia (a configuration that must be extremely rare,

Table 2 New classification

Classification LIS group	Classification (genotype)	Gene defect	Role	Pattern of inheritance	Brain MRI	Pathology	OMIM resource
Classic LIS	*LIS1*	17p13.3 (PAFAH1B1) 14-3-3ε (Miller–Dieker syndrome)	Gene encoding platelet activating factor acetylhydrolase 1 subunit B1 (PAFAH1B1) assembling microtubules and leading neuronal migration (cell nucleus migration, generation of neuroblast and cell survival)	A	Smooth brain; agyria; pachygyria (15- to 20-mm thickness); SCBH; worse posteriorly (P > A)	Four-layered cortex	607432
	LIS1 mosaicism	Somatic mosaicism (R241P-R8X)	Same mutation as LIS1 but two cell populations have distinct genotypes	A	Less severe involvement than LIS1	Four-layered cortex	607432
	DCX (*XLIS*)	Xq22.3-q23	Gene encoding doublecortin (DCX), leading edge of the cells during neuronal migration	XLD	Smooth brain; agyria; pachygyria (15- to 20-mm thickness); SCBH; worse anteriorly (A > P) in hemizygous males; milder involvement or only SCBH in heterozygous females	Four-layered cortex	300067
Variant LIS	*ARX* (*XLAG*)	Xp22.13	Probably encoding for a protein involved in migration and differentiation of interneurons containing γ-aminobutyric acid (GABAergic interneurons)	XLR	Smooth brain; pachygyria A > P (6–7 mm < thickness < 10 mm); posterior agyria; basal ganglia and white matter anomalies; ACC	Three-layered cortex	300215
	RELN (similar to Norman-Roberts type)	7q22	Gene encoding reelin (RELN), leading disengagement of migrating neurons from radial glial cells	A	Smooth brain; thickened cortex (10 mm) A > P; hippocampal abnormalities; severe mid-hindbrain involvement	*	257320
	VLDLR (including HDS)	9p24	RELN binds directly and specifically to the extracellular domains of VLDLR and ApoER2-Reelin acts via VLDLR and ApoER2 to guide neuroblast migration in the cerebral cortex and cerebellum	AR	Similar to RELN or thick cortex with simplified gyral pattern	ND	192977 224050
	ND1	ND	ND	ND	Entire brain agyria; subependymal linear heterotopia; ACC; severe mid-hindbrain involvement	Four-layered cortex	Miyata et al. *Acta Neuropathol* 2004; 107:69-81†
	ND2	ND	ND	ND	Entire brain pachygyria; undulating band heterotopia; ACC	ND	None
	ND3 (similar to Baraitser-Winter syndrome)	inv p12q14 (PAX8)	PAX 8 maps to chrom 2 and controls the differentiation of primordial cells and is involved in organogenesis	Sporadic	Microcephaly; paracentral pachygyria; CSZ; ACC	ND	243310
	TL-LIS (two-layered LIS)	ND	ND	ND	Entire brain pachygyria with no gradient; disorganized neurons	Two-layered cortex	Forman et al. *J Neuropathol Exp Neurol* 2005;64: 847-857†

—*Continued*

Table 2 *Continued*

Classification LIS group	Classification (genotype)	Gene defect	Role	Pattern of inheritance	Brain MRI	Pathology	OMIM resource
Cobblestone complex	*FCMD* (Fukuyama type and similars)	9q31-q33 (FKRP)	Mutation in the gene encoding fukutin-related protein (FKRP), which probably participates in the pathway of biosynthesis of dystroglycan involved in binding activity for the ligand laminin	AR	Thick cortex with frontal polymicrogyria; temporo-occipital cobblestone cortex; irregular inner surface with bundles of neurons crossing radially to subpial spaces; smooth outer surface; subcortical cysts; leukodystrophy	Unlayered frontal polymicrogyria; bundles of neurons separated by fibroglial vascular tissue extending radially through the cortex into subarachnoid spaces (cobblestone cortex); irregular gray–white matter junction; dysplasia; leptomeningeal cysts	253800
	WWS	19q13.3, 14q24.3 (POMT2), 9q34.1 (POMT1), 9q31 (FKRP)	Gene encoding protein *O*-mannosyltransferase-1 (POMT1) involved in *O*-mannose–linked glycosylation of proteins important for the formation of glial limiting membrane	AR	Cobblestone cortex; hydrocephalus; retinal dysplasia; leukodystrophy; severe brainstem and cerebellum hypoplasia; mid-hindbrain junction dorsal kink	Cobblestone cortex	236670
	MEB	19q13.3, 1p34-p33 (POMGnT1)	Mutations in *O*-mannose β-1,2-*N*-acetylglucosaminyltransferase (POMGnT1), which participates in *O*-mannosyl glycan synthesis, results in disorder of radial migration and disruption of the pial barrier	AR	Same features but intermediate severity between FCMD and WWS	Cobblestone cortex	253280
Related muscular dystrophy syndromes	*CMD* Merosin deficiency	6q22-q23	Mutation in the laminin α2 gene (LAMA2), which is a permissive substrate for migration of oligodendrocyte precursors	AD	Occipital agyria (no cobblestone cortex); striking leukodystrophy involving U fibers; pontocerebellar hypoplasia; cerebellar cysts	Same as LIS1 in affected occipital cortex?	607855

Proposal adapted from Forman et al.,[3] including all lissencephaly (LIS) types and details from Online Mendelian Inheritance in Man (OMIM) resources.
*No pathology described.
†No OMIM resource.
A = autosomal; XLD = X-linked dominant; XLR = X-linked recessive; AR = autosomal recessive; ND = not determined; AD = autosomal dominant; SCBH = subcortical band heterotopia; ACC = agenesis of corpus callosum; CSZ = cell-sparse zone; FCMD = Fukuyama congenital muscular dystrophy; WWS = Walker-Warburg syndrome.

because we found no previous reports) and ACC. ND1 refers to two cases with complete agyria, SELH, ACC, and severe MHB involvement. Further investigations or more cases are needed to determine whether the ND groups should be classified with vLIS or in still another category.

As noted in the previous paragraph, it was difficult to determine which entities to include in the vLIS category and how to classify them. More than 80% of vLIS patients did not have characteristic imaging findings (ND). The protein products of *VLDLR* and *RELN* act in the same pathway but are coded by different genes that have different patterns of inheritance, so they were included as separate malformations. Based on a previously cited work, we included two-layered lissencephaly as part of the vLIS category.[3]

Another weakness of this study is a lack of clinical data that could help clinicians to better identify patients with these malformations. It would also have helped to better classify those patients who were ultimately assigned to the ND category. Despite this obvious deficiency, important information has emerged from this study for both radiologists and other physicians interested in brain development. This study expands the categories of lissencephalies and adds to the knowledge of associated malformations. This information will, hopefully, lead to further studies of the molecular disorders involved in the many brain anomalies associated with agyria and pachygyria and, ultimately, a better understanding of the mechanisms by which the brain is formed.

AUTHOR CONTRIBUTIONS

P.J.-T. conducted the statistical analysis.

ACKNOWLEDGMENT

The authors thank Drs. Chistopher Walsh, William Dobyns, Daniela Pilz, Sean Bryant, and Naci Koçer for the MRI scans that they kindly contributed to this work.

Received March 7, 2008. Accepted in final form July 16, 2008.

REFERENCES

1. Barkovich AJ. Congenital malformations of the brain and skull. In: Pediatric Neuroimaging, 4th ed. Philadelphia: Lippincott Williams & Wilkins; 2005.
2. Kato M, Dobyns WB. Lissencephaly and the molecular basis of neuronal migration. Hum Mol Genet 2003;12: R89–R96.
3. Forman MS, Squier W, Dobyns WB, et al. Genotypically defined lissencephalies show distinct pathologies. J Neuropathol Exp Neurol 2005;64:847–857.
4. Dobyns WB, Truwit CL, Ross ME, et al. Differences in the gyral pattern distinguish chromosome 17-linked and X-linked lissencephaly. Neurology 1999;53:270–277.
5. Dobyns WB, Reiner O, Carrozzo R, et al. Lissencephaly: a human brain malformation associated with deletion of the

LIS1 gene located at chromosome 17p13. JAMA 1993; 270:2838–2842.
6. Ross ME, Swanson K, Dobyns WB. Lissencephaly with cerebellar hypoplasia (LCH): a heterogeneous group of cortical malformations. Neuropediatrics 2001;32:256–263.
7. van der Knaap MS, Smit LM, Barth PG, et al. Magnetic resonance imaging in classification of congenital muscular dystrophies with brain abnormalities. Ann Neurol 1997; 42:50–59.
8. Aida N, Tamagawa K, Takada K, et al. Brain MR in Fukuyama congenital muscular dystrophy. AJNR Am J Neuroradiol 1996;17:605–613.
9. Valanne L, Pihko H, Katevuo K, et al. MRI of the brain in muscle-eye-brain (MEB) disease. Neuroradiology 1994; 36:473–476.
10. Mercuri E, Topaloglu H, Brockington M, et al. Spectrum of brain changes in patients with congenital muscular dystrophy and FKRP gene mutations. Arch Neurol 2006;63: 251–257.
11. Vajsar J, Schachter H. Walker-Warburg syndrome. Orphanet J Rare Dis 2006;29:1–5.
12. Barkovich AJ, Kuzniecky RI, Jackson GD, et al. A developmental and genetic classification for malformations of cortical development. Neurology 2005;65:1873–1887.
13. Schurig V, Orman AV, Bowen P. Nonprogressive cerebellar disorder with mental retardation and autosomal recessive inheritance in Hutterites. Am J Med Genet 1981;9: 43–53.
14. Boycott KM, Flavelle S, Bureau A, et al. Homozygous deletion of the very low density lipoprotein receptor gene causes autosomal recessive cerebellar hypoplasia with cerebral gyral simplification. Am J Hum Genet 2005;77:477–483.
15. Leite CC, Lucato LT, Martin MGM. Merosin-deficient congenital muscular dystrophy (CMD): a study of 25 Brazilian patients using MRI. Pediatr Radiol 2005;35:572–579.
16. Philpot J, Pennock J, Cowan F, et al. Brain magnetic resonance imaging abnormalities in merosin-positive congenital muscular dystrophy. Eur J Paediatr Neurol 2000;4:109–114.
17. Hong SE, Shugart YY, Huang DT, et al. Autosomal recessive lissencephaly with cerebellar hypoplasia is associated with human RELN mutations. Nat Genet 2000;26:93–96.
18. Glass HC, Boycott KM, Adams C, et al. Autosomal recessive cerebellar hypoplasia in the Hutterite population. Dev Med Child Neurol 2005;47:691–695.
19. Longman C, Brockington M, Torelli S, et al. Mutations in the human LARGE gene cause MDC1D, a novel form of congenital muscular dystrophy with severe mental retardation and abnormal glycosylation of alpha-dystroglycan. Hum Mol Genet 2003;12:2853–2861.
20. Beltran-Valero de Bernabé D, Voit T, Longman C, et al. Mutations in the FKRP gene can cause muscle-eye-brain disease and Walker-Warburg syndrome. J Med Genet 2004;41:e61.
21. van Reeuwijk J, Janssen M, van den Elzen C, et al. POMT2 mutations cause alpha-dystroglycan hypoglycosylation and Walker-Warburg syndrome. J Med Genet 2005;42:907–912.
22. van Reeuwijk J, Maugenre S, van den Elzen C, et al. The expanding phenotype of POMT1 mutations: from Walker-Warburg syndrome to congenital muscular dystrophy, microcephaly, and mental retardation. Hum Mutat 2006;27:453–459.
23. van Reeuwijk J, Grewal PK, Salih MA, et al. Intragenic deletion in the LARGE gene causes Walker-Warburg syndrome. Hum Genet 2007;121:685–690.
24. Qu Q, Crandall JE, Luo T, et al. Defects in tangential neuronal migration of pontine nuclei neurons in the Largemyd mouse are associated with stalled migration in the ventrolateral hindbrain. Eur J Neurosci 2006; 23:2877–2886.
25. Barkovich AJ, Millen KJ, Dobyns WB. A developmental classification of malformations of the brainstem. Ann Neurol 2007;62:625–639.
26. Dobyns WB, Berry-Kravis E, Havernick NJ, et al. X-linked lissencephaly with absent corpus callosum and ambiguous genitalia. Am J Med Genet 1999;86:331–337.
27. Paul LK, Brown WS, Adolphs R, et al. Agenesis of the corpus callosum: genetic, developmental and functional aspects of connectivity. Nat Rev Neurosci 2007;8:287–299.
28. Dobyns WB. Absence makes the search grow longer. Am J Hum Genet 1996;58:7–16.
29. Kappeler C, Dhenain M, Tuy FPD, et al. Magnetic resonance imaging and histological studies of corpus callosal and hippocampal abnormalities linked to doublecortin deficiency. J Comp Neurol 2007;500:239–254.
30. Ganesh A, Al-Kindi A, Jain R, Raeburn S. The phenotypic spectrum of Baraitser-Winter Syndrome: a new case and review of literature. J AAPOS 2005;9:604–606.